Title

Studies on the Enantioselective Iminium Ion Trapping of Radicals Triggered by an Electron-Relay Mechanism

Journal

Journal of the American Chemical Society, 139(12)

ISSN

0002-7863

Authors

Bahamonde, Ana
Murphy, John J
Savarese, Marika
et al.

Publication Date

2017-03-29

DOI

10.1021/jacs.7b01446

JACS
JOURNAL OF THE AMERICAN CHEMICAL SOCIETY
Article
pubs.acs.org/JACS

Studies on the Enantioselective Iminium Ion Trapping of Radicals Triggered by an Electron-Relay Mechanism

Ana Bahamonde,[†] John J. Murphy,[†] Marika Savarese,[‡] Éric Brémond,[‡] Andrea Cavalli,[‡,⊥] and Paolo Melchiorre*[,†,§]

[†]ICIQ - Institute of Chemical Research of Catalonia, The Barcelona Institute of Science and Technology, Avinguda Països Catalans 16, 43007 Tarragona, Spain

[‡]D3 CompuNet, Istituto Italiano di Tecnologia, via Morego 30, 16163 Genova, Italy

[§]ICREA, Passeig Lluís Companys 23, 08010 Barcelona, Spain

[⊥]Dept. of Pharmacy and Biotechnology, via Belmeloro 6, 40126 Bologna, Italy

Supporting Information

ABSTRACT: A combination of electrochemical, spectroscopic, computational, and kinetic studies has been used to elucidate the key mechanistic aspects of the previously reported enantioselective iminium ion trapping of photochemically generated carbon-centered radicals. The process, which provides a direct way to forge quaternary stereocenters with high fidelity, relies on the interplay of two distinct catalytic cycles: the aminocatalytic electron-relay system, which triggers the stereoselective radical trap upon iminium ion formation, and the photoredox cycle, which generates radicals under mild conditions. Critical to reaction development was the use of a chiral amine catalyst, bearing a redox-active carbazole unit, which could rapidly reduce the highly reactive and unstable intermediate generated upon radical interception. The carbazole unit, however, is also involved in another step of the electron-relay mechanism: the transiently generated carbazole radical cation acts as an oxidant to return the photocatalyst into the original state. By means of kinetic and spectroscopic studies, we have identified the last redox event as being the turnover-limiting step of the overall process. This mechanistic framework is corroborated by the linear correlation between the reaction rate and the reduction potential of the carbazole unit tethered to the aminocatalyst. The redox properties of the carbazole unit can thus be rationally tuned to improve catalytic activity. This knowledge may open a path for the mechanistically driven design of the next generation of electron-relay catalysts.

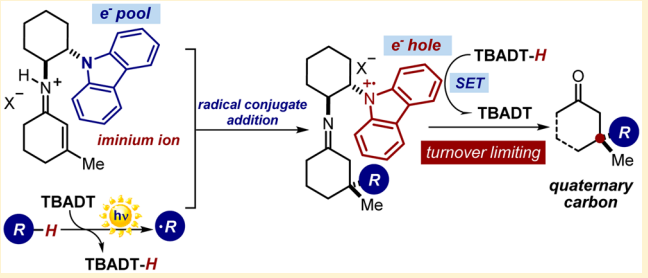

INTRODUCTION

Iminium ion activation[1] is an established strategy of modern organic chemistry for effectively synthesizing enantio-enriched chiral molecules. The approach exploits the capacity of chiral primary or secondary amines to reversibly condense with unmodified α,β-unsaturated carbonyl compounds to form iminium ion intermediates **A** (Figure 1a). The electronic redistribution within **A**, by lowering the energy of the lowest unoccupied molecular orbital (LUMO), facilitates conjugate additions of soft nucleophiles to the β-carbon atom. At the same time, the chiral amine fragment dictates the stereochemistry of the final β-functionalized products. This catalytic platform has found many applications in the polar domain over the past 15 years,[2] effectively complementing established metal-based asymmetric strategies for conjugate additions to unsaturated carbonyl compounds.[3] However, chiral iminium ions **A** have never been used to stereoselectively trap nucleophilic radicals. This is surprising given the strong tendency of open-shell species to react with electron-deficient olefins.[4]

Recently, our laboratories reported a strategy to fill this gap in catalytic enantioselective methodology. We showed that the applicability of iminium ion activation is not limited to two-electron reaction manifolds. Rather, it can be successfully expanded to include radical reactivity domains.[5] Synthetically, the chemistry provided a catalytic method to forge quaternary carbon stereocenters[6] with high fidelity by means of an enantioselective radical conjugate addition (RCA)[7−9] to β-disubstituted enones **1** (Figure 1b).

In successfully realizing a stereocontrolled iminium ion trapping of radicals, one factor was crucial: the design of a chiral amine catalyst, purposely adorned with a *carbazole redox-active* moiety. Our design plan was motivated by the instability of the α-iminyl radical cation **B**, a short-lived intermediate generated upon radical addition to the cationic iminium ion **A** (Figure 2a). In consonance with the classical behavior of radical ions,[10] intermediate **B** has a high tendency to undergo radical elimination (β-scission),[11] thus reforming the more stable

Received: February 10, 2017
Published: March 10, 2017

DOI: 10.1021/jacs.7b01446
J. Am. Chem. Soc. XXXX, XXX, XXX−XXX

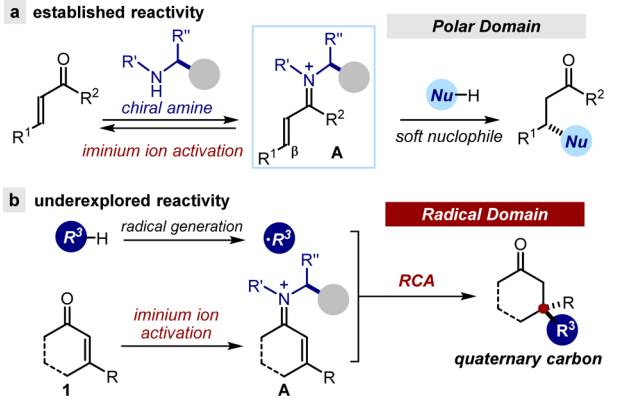

Figure 1. Iminium-ion-mediated catalysis: (a) Established polar reactivity of chiral iminium ions **A** in enantioselective conjugate additions of soft nucleophiles. (b) Radical conjugate addition (RCA) to chiral iminium ions **A** catalytically generated from β-disubstituted enones **1** to forge quaternary stereocenters; filled gray circle represents a bulky substituent on the chiral amine catalyst.

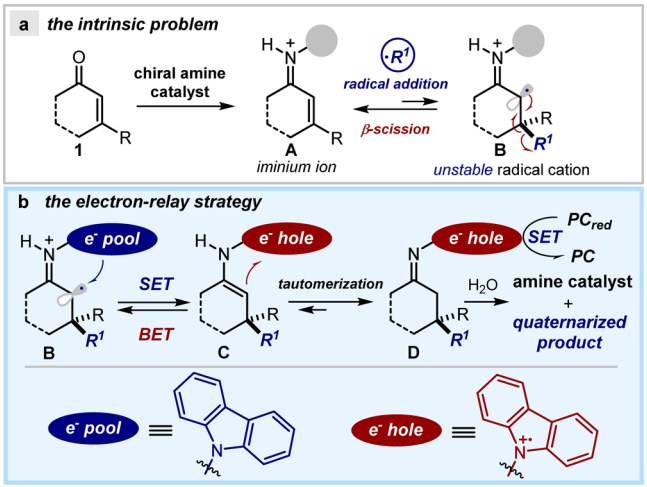

Figure 2. (a) Challenges associated with implementing the iminium-ion-catalyzed conjugate additions of radicals ($^{\bullet}R^1$); the gray circle represents the chiral organic catalyst scaffold. (b) The electron-relay strategy to bypass the short-lived α-iminyl radical cation **B** by intramolecular reduction, and the role of tautomerization to prevent back-electron transfer. SET = single-electron transfer, BET = back-electron transfer, ***PC*** = photocatalyst, PC_{red} = reduced form of the photocatalyst. The blue ellipse represents the electron-rich reducing carbazole moiety, while the magenta ellipse represents the persistent carbazole radical cation.

conjugated iminium ion **A**. We recognized that the main obstacle to reaction development was the high reactivity and fleeting nature of the distonic radical **B**.

Our main idea for taming this troublesome intermediate was to tether an electron-rich carbazole moiety (*electron pool* unit in Figure 2b) at a strategic position on the organocatalyst where it is poised to undergo a very rapid intramolecular single-electron transfer (SET) reduction of the unstable species **B**, preventing it from breaking down. The nascent enamine intermediate **C** then tautomerizes to form the more stable imine **D**,[12] thus avoiding a possible competitive back-electron transfer (BET). Finally, the carbazole radical cation (*electron hole* unit within **D**), arising from the intramolecular SET event, undergoes single-electron reduction from the photoredox catalyst. This restores the neutral carbazole moiety while yielding the quaternary product and releasing the original organocatalyst. Notably, a photocatalyst (***PC*** in Figure 2b) both creates the nucleophilic radical and promotes the final SET event (full mechanistic details in Figure 4, below). Overall, in this catalytic system, the carbazole unit serves as an *electron-relay center*, since it behaves alternately as an acceptor and a donor to shuttle electrons.[13] First, the excellent electron-donating capabilities of the carbazole trigger a fast proximity-driven intramolecular reduction of **B**.[14] Meanwhile, the kinetic stability of the long-lived carbazole radical cation in **D** allows for a productive intermolecular SET reduction from the reduced photocatalyst (PC_{red} in Figure 2b).[15]

The effectiveness of this *electron-relay mechanism* was initially demonstrated in the reaction between the commercially available β-methyl cyclohexenone **1a** and benzodioxole **2a** (Figure 3a).[5] We used the inorganic photocatalyst tetrabuty-

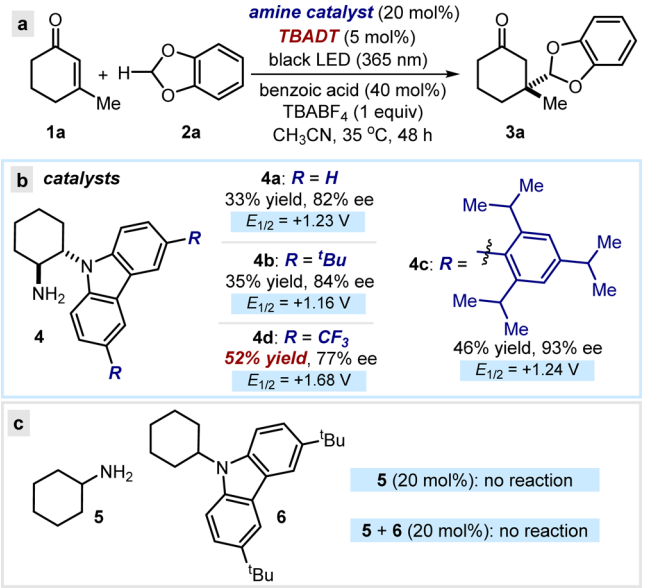

Figure 3. (a) The model reaction to test the feasibility of the electron-relay strategy. (b) The unanticipated effect that the redox properties of the carbazole-based primary amine catalysts **4** have on the reactivity. $E_{1/2}$ is the reduction potential of the carbazole-based catalysts **4a–d** as measured by cyclic voltammetry vs Ag/Ag^+ in CH_3CN; the carbazole within **4** undergoes a reversible oxidation to produce the corresponding carbazoliumyl radical cation. (c) Experiments suggesting that, to make the electron-relay mechanism operative, there needs to be close spatial proximity between the iminium ion handle and the redox active carbazole moiety.

lammonium decatungstate[16] (TBADT, 5 mol%). Upon light excitation, TBADT can easily photogenerate a nucleophilic carbon-centered radical by homolytically cleaving the methylene C–H bond in **2a**[17] via a hydrogen-transfer mechanism (HAT). The experiments were conducted at 35 °C in acetonitrile (CH_3CN) and under irradiation by a single black-light-emitting diode (black LED, λ_{max} = 365 nm).

The chiral cyclohexylamine catalyst **4a**, adorned with the carbazole moiety, provided the desired product **3a** with appreciable yield and stereoselectivity (33% yield, 82% ee, Figure 3b). In consonance with the proposed electron-relay mechanism, the reaction could not be catalyzed by simple cyclohexylamine **5** (20 mol%), which mimics the catalyst's **4a** scaffold while lacking the redox-active moiety (Figure 3c). Also,

DOI: 10.1021/jacs.7b01446
J. Am. Chem. Soc. XXXX, XXX, XXX–XXX

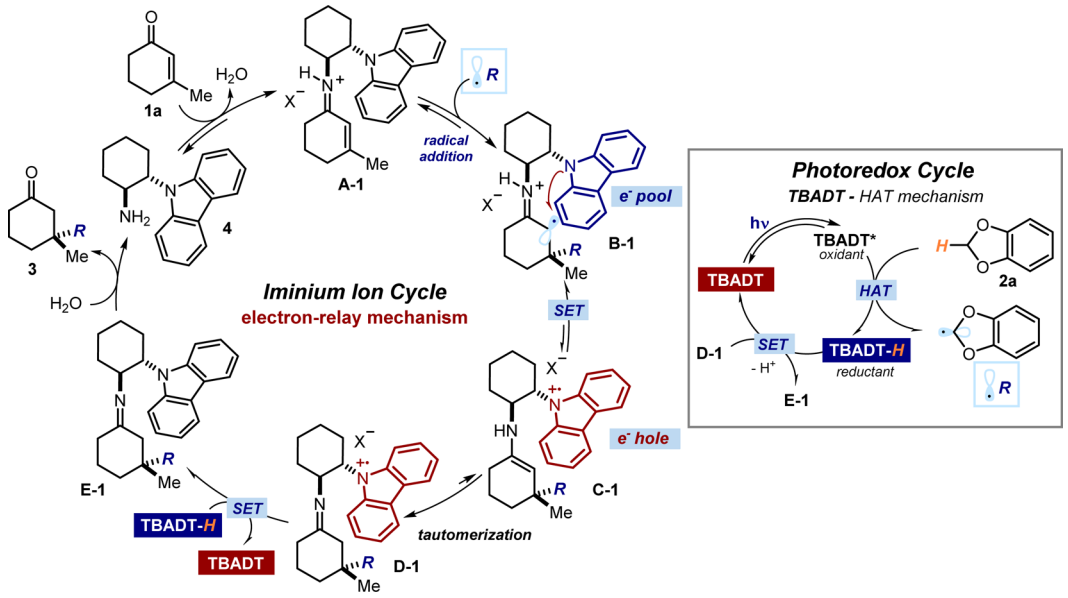

Figure 4. Electron-relay mechanism underlying the iminium-ion-mediated enantioselective radical conjugate addition to enone **1a**. Upon radical addition to the iminium ion **A-1**, the electron-relay mechanism bypasses the unstable distonic radical **B-1** producing a carbazoliumyl radical cation **C-1**, which is prevented from undergoing back-electron transfer by tautomerization of the secondary enamine to the corresponding imine **D-1**. The redox-active carbazole unit plays two critical roles: (*i*) the carbazole acts as a reducing agent to transform the short-lived α-iminyl radical cation **B-1** into the stable enamine **C-1** upon *intramolecular SET reduction*; (*ii*) the long-lived carbazoliumyl radical cation in **D-1** regenerates the photocatalyst (TBADT) by *intermolecular SET oxidation* of the reduced form (TBADT-H), affording the neutral imine **E-1**, which eventually hydrolyzes to liberate the aminocatalyst **4**. The gray rectangle shows the TBADT-mediated photoredox cycle, which affords the carbon-centered radical from benzodioxole precursors **2** by means of a HAT mechanism. SET = single-electron transfer, HAT = hydrogen-atom transfer.

an equimolar combination of cyclohexylamine **5** and exogenous *N*-cyclohexyl 3,6-di-*tert*-butyl-carbazole **6** (20 mol%) proved unsuitable for catalysis, indicating the importance of a proximity-driven intramolecular SET process to reduce the unstable α-iminyl radical cation **B**.

However, during the optimization campaign, we came across an unanticipated effect of the redox properties of the carbazole scaffold within the amine catalysts **4** on the reaction rate (Figure 3b). When modifying the redox-active carbazole by introducing substituents of different electronic nature at the 3- and 6-positions,[18] we expected the presence of electron-donating groups to accelerate the overall RCA process. This is because an increase in electron density within the carbazole electron pool should facilitate the SET reduction of intermediate **B**, a step that we envisioned would be crucial for reactivity (Figure 2b). In contrast, catalyst **4d**, bearing a CF_3 electron-withdrawing group at the 3,6-positions of the carbazole which depletes the electron pool, was considerably more active than the more reducing catalyst **4b** and **4c** (results in Figure 3b). The redox potentials of catalysts **4a**–**d**, as measured by cyclic voltammetry vs Ag/Ag^+ in CH_3CN ($E_{1/2}$(**4b**) = +1.16 V; $E_{1/2}$(**4c**) = +1.24 V; and $E_{1/2}$(**4d**) = +1.68 V, where $E_{1/2}$ is the reduction potential of the carbazole unit undergoing a reversible oxidation to produce the corresponding carbazoliumyl radical cation), further indicated that the catalyst **4d**, bearing the less reducing carbazole, displayed the highest catalytic activity. This unexpected result[19] challenged our understanding of the reaction mechanism and prompted us to undertake extensive mechanistic investigations.

Herein, we detail how a combination of physical organic techniques, including electrochemical and kinetic studies, allowed us to rationalize the effects the electronic properties of the redox-active carbazole unit have on the reaction rate. These investigations revealed an unanticipated turnover-limiting step. They also confirmed the importance of the proposed electron-relay mechanism in triggering the enantioselective iminium ion trapping of photochemically generated radicals.

RESULTS AND DISCUSSION

Figure 4 presents a detailed description of the proposed mechanism for the iminium-ion-mediated RCA, which is characterized by the synergistic activities of two intertwined manifolds: the iminium ion and the photoredox catalytic cycles. It is important to note that a radical chain mechanism is not possible in this system. This is because generating a radical from substrate **2a** requires a HAT mechanism, while the feasibility of a chain propagation sequence could only rely on the oxidation ability of the carbazole radical cation within intermediate **D-1**, which could manifest itself exclusively through an outer-sphere SET manifold.

The notion that the CF_3-containing catalyst **4d** offered an improved reactivity in the model reaction was dissonant with our mechanistic hypothesis that an easier reduction of the short-lived α-iminyl radical cation **B-1** would facilitate the reaction (see reactivity trend in Figure 3b). Indeed, this step should be hampered by an electron-poor carbazole unit. However, the intramolecular SET reduction of **B-1** to give the enamine intermediate **C-1** is not the only electron-relay step in which the redox-active carbazole unit is involved. The carbazole radical cation in the imine **D-1**, arising from the tautomerization of the secondary enamine **C-1**, acts as an oxidant of the reduced photocatalyst (TBADT-H). This bimolecular SET event is essential to restore the neutral carbazole moiety within **E-1** while closing the photoredox cycle, returning the TBADT catalyst in the original state. This step could be facilitated by an electron-poor substituent which

DOI: 10.1021/jacs.7b01446
J. Am. Chem. Soc. XXXX, XXX, XXX−XXX

magnifies the oxidizing power of the carbazole radical cation in **D-1**. We performed detailed kinetic studies to assess the relative importance of the two SET steps of the electron-relay mechanism (intramolecular reduction of **B-1** to afford the carbazole radical cation and regeneration of the neutral carbazole unit in **E-1** by intermolecular SET) and their influence on the overall reactivity.

Kinetic Studies. As the model for the kinetic studies, we chose the reaction between the commercially available β-methyl cyclohexenone **1a** and 2-methyl benzodioxole **2b** to afford the radical conjugate addition product **3b** (Scheme 1). This

Scheme 1. Model Reaction for the Kinetic Investigations[a]

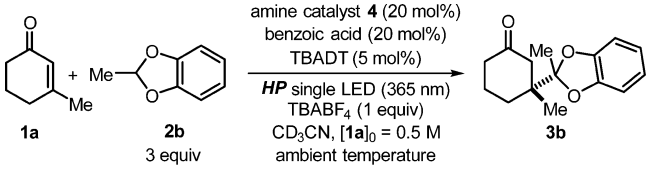

[a]Reactions conducted under irradiation from a high-power (HP) single black-light-emitting diode (black LED, λ_{max} = 365 nm). [**4**] = 0.1 M, [**1a**] = 0.5 M, [**2a**] = 1.5 M, [TBADT] = 0.025 M, [$TBABF_4$] = 0.5 M and [benzoic acid] = 0.1 M. $TBABF_4$ = tetrabutylammonium tetrafluoroborate.

decision was based on the complete lack of reactivity observed in the absence of the chiral aminocatalyst of type **4**,[20] which precluded any background process from altering the kinetic analysis.

The experiments were conducted at ambient temperature in the presence of the carbazole-based aminocatalyst **4** (20 mol%), TBADT (5 mol%), benzoic acid (20 mol%, to facilitate iminium ion formation),[21] and an excess of radical precursor **2b** (3 equiv). Deuterated acetonitrile (CD_3CN) was used as the solvent for it secured full substrate solubility and homogeneity of the system. We applied the method of initial-rate kinetics, monitoring the progress of the reactions by ^1H NMR analysis and following the conversion until 15%. The initial rates were plotted against concentration to obtain straight lines (see Section D in the Supporting Information for details). Our initial-rate kinetic studies required an independent reaction to be performed for every data-point at different times.

First, we evaluated the influence of the light intensity on the rate of the model reaction detailed in Scheme 1 and catalyzed by the chiral amine **4b** (Figure 5). For the illumination system,

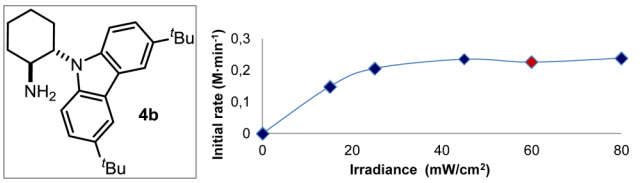

Figure 5. Light intensity/reactivity correlation studies. Model reactions conducted as specified in Scheme 1 and catalyzed by **4b**.

we used a single high-power (HP) black-light-emitting diode (black LED, λ_{max} = 365 nm) connected to an external power supply, which allowed us to finely tune and control the intensity of light emission. The irradiance was carefully measured with a photodiode light detector at the start of each reaction. To secure a reliable and consistent irradiation throughout the kinetic investigation, we used a setup that maintained a constant distance of 1.5 cm between the reaction vessel and the light source (full details in Figure S1). The rate of the model reaction catalyzed by **4b** was found to linearly correlate with the light intensity, flattening out for irradiances higher than 40 mW/cm^2. Under this regime, where the reaction is not light-limited, the overwhelming majority of the TBADT photocatalyst could be opportunely excited. Considering the light intensity/reactivity correlation depicted in Figure 5, all the following kinetic studies were performed using the setup discussed above and an illumination system (HP black LED, λ_{max} = 365 nm) with an irradiance of 60 ± 2 mW/cm^2. This ensured the reactions were not light-limited.

We then focused on the unexpected observation that the catalytic activities of catalysts **4a–d**, as detailed in Figure 2b, inversely correlated with the reducing power of the carbazole unit. Specifically, we wondered whether the electronic properties of the chiral catalysts were solely responsible for the different reactivities, since steric effects could also influence the reaction rate. For example, the data in Figure 2b clearly indicated how the steric profile of the carbazole substituents in catalysts **4a–d** was strongly connected with the level of stereoinduction in the RCA process. To clearly differentiate the electronic and steric effects, a new family of catalysts, containing *para*-substituted aryl moieties at the 3,6-carbazole positions, was synthesized (catalysts **4e–h**, Figure 6a).

The *para*-substitution pattern was carefully chosen to provide the redox-active carbazole unit with a wide range of electronic properties but a comparable steric shielding ability. In consonance with this design plan, catalysts **4e–h** all promoted the model reaction to afford the product **3b** with the same level of stereocontrol (in the range of 87–88% of enantiomeric excess, ee), thus demonstrating that a comparable chiral environment and shielding effect was created at the remote β-carbon of the reactive iminium ion intermediate.[22] These results suggested that the *para*-substituted 3,6-aryl carbazole catalysts **4e–h** are characterized by a similar steric profile, and that possible differences in reaction rate should arise from electronic factors exclusively.

On this basis, we explored how varying the electronic properties of the chiral carbazole catalysts **4e–h** affected the rate of the model reaction depicted in Scheme 1, discounting any steric contribution. Applying the method of initial-rate kinetics, we confirmed that catalysts bearing more electron-withdrawing groups within the carbazole unit imparted a higher rate, with catalyst **4f** providing the faster reaction. In addition, we observed a positive linear correlation between the rate constants and the Hammett σ_{para} value of the aryl moiety in catalysts **4e–h**. Figure 6b shows the linear free-energy relationship (LFER)[23] between the electronics of the carbazole unit within catalysts **4** and the rate constant of the catalyzed reaction.

Since the electronic properties directly influence the redox power of the carbazole unit, it is unsurprising that the observed initial rates also correlated linearly with the redox potentials of aminocatalysts **4e–h**, measured electrochemically by cyclic voltammetry vs Ag/Ag^+ in CH_3CN (Figure 6c). A linear relationship also persisted between the catalyst redox potentials and the σ_{para} value of the *para*-substituted aryl substituents (Figure 6d). In principle, this correlation provides a way to predict[24] both the electrochemical potential and the catalytic activity of new members of the *para*-substituted 3,6-aryl carbazole catalyst family.

DOI: 10.1021/jacs.7b01446
J. Am. Chem. Soc. XXXX, XXX, XXX–XXX

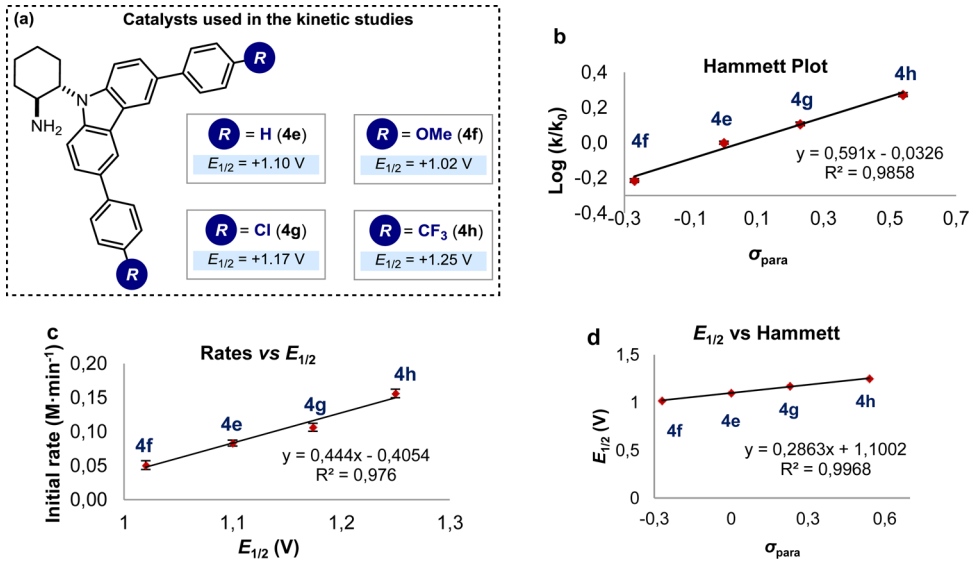

Figure 6. (a) A new family of chiral catalysts: *para*-substituted 3,6-aryl carbazole catalysts **4e–h**. They promoted the model reaction depicted in Scheme 1 inferring the same level of stereoselectivity (87–88% ee). $E_{1/2}$ is the reduction potential of the carbazole-based catalysts **4e–h** as measured by cyclic voltammetry vs Ag/Ag^+ in CH_3CN; the carbazole within **4** undergoes a reversible oxidation to produce the corresponding carbazoliumyl radical cation. (b) LFER correlating the Hammett σ value of the *para*-substituted aryl carbazole moiety with the initial rates for the model reaction depicted in Scheme 1 catalyzed by catalysts **4e–h**. (c) Correlations between the initial rates and the redox potentials measured for the different aminocatalysts **4e–h**. (d) Linear relationship between the redox potentials for the different aminocatalysts and the corresponding Hammett σ value of their aryl moiety. Reactions performed in CD_3CN under illumination by HP black LED, λ_{max} = 365 nm, with an irradiance of 60 ± 2 mW/cm^2. [**4**] = 0.1 M, [**1a**] = 0.5 M, [**2a**] = 1.5 M, [TBADT] = 0.025 M, [$TBABF_4$] = 0.5 M and [benzoic acid] = 0.1 M. The error bars in (c) represent the standard deviation.

Collectively, these results indicate that the electronic properties of the catalyst carbazole unit, which are strictly correlated with their redox abilities, strongly influence the rate of the model reaction. Specifically, the larger the reduction potential of the carbazole tethered to the aminocatalyst, the faster the reaction proceeds. To fully rationalize this redox properties/reactivity relationship, we undertook a reaction-profile analysis and rate-order assessment to establish the turnover-limiting step. Initial-rate kinetic investigations of the model reaction depicted in Scheme 1 were performed across a range of concentrations for each reaction component. In these studies, we used an illumination system (HP black LED, λ_{max} = 365 nm) with an irradiance of 60 ± 2 mW/cm^2 to ensure that the processes were not light-limited. Two independent series of kinetic investigations were performed using carbazole-based aminocatalysts **4b** and **4e**, which provided similar and reproducible kinetic profiles. This was done to ensure that similar trends could be observed when using catalysts with different architectures and steric profiles on the redox active carbazole unit.

Figure 7 details the results of our initial-rate kinetic investigations. The reaction was found to be first order in the catalyst (both amines **4b** and **4e**). No order was observed in 2-methyl benzodioxole **2b**, the radical precursor. Interestingly, when the β-methyl cyclohexenone **1a** dependence was investigated, the rate dependence was found to be curved, showing a saturation kinetic profile. This behavior indicates that the amine catalyst **4** is partitioned between the free-state and the iminium ion intermediate **A-1**.

To corroborate this scenario, we used ^{1}H NMR spectroscopy to investigate the equilibrium of iminium ion formation under the conditions used in the kinetic experiments (Figure 8). The protonated free catalyst **4b**·$PhCO_2H$, the imine **F-1**, and the iminium ion **A-1** were detected in a ratio of 1:0.3:1.3, respectively. These spectroscopic studies are consonant with the notion that it is not possible to identify a definitive resting state for catalyst **4b**, with the catalyst concentration being shared between different closed-shell intermediates.

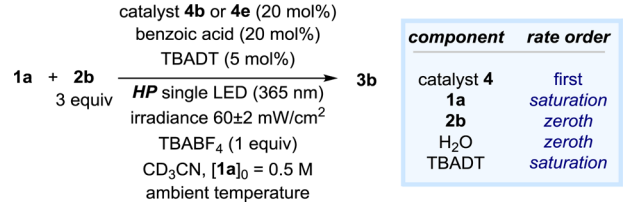

Figure 7. Model reaction used for initial-rate kinetics and the observed rate orders. Conversions determined by ^{1}H NMR analysis. Studies performed across a range of concentrations for each reaction component in CD_3CN. The kinetic studies were repeated twice using amines **4b** and **4e** to catalyze the model transformation; both studies gave similar kinetic profiles.

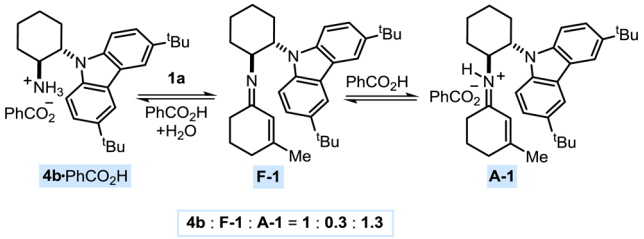

Figure 8. Partitioning of the chiral amine catalyst **4b** between different intermediates and the formation of the iminium ion **A-1** under the reaction conditions used for the kinetic studies. ^{1}H NMR experiments performed in anhydrous CD_3CN at 298 K with [**4b**] = 0.1 M, [**1a**] = 0.5 M, [**2a**] = 1.5 M, [TBADT] = 0.025 M, [NBu_4BF_4] = 0.5 M, and [benzoic acid] = 0.1 M. The experiment was conducted in the dark.

DOI: 10.1021/jacs.7b01446
J. Am. Chem. Soc. XXXX, XXX, XXX–XXX

In principle, the amount of water in solution might influence the formation of the iminium ion **A-1**. We thus explored the effect of water on the rate of the model reaction. No alteration of the kinetic profile was observed after the addition of either 1 or 5 equiv of H_2O. These results indicate that the turnover is not limited by either the iminium ion **A-1** formation or the hydrolysis of the imine intermediate **E-1**, which leads to the alkylation product **3b** while liberating the catalyst **4** (see Figure 4 for the full mechanistic picture).

The zeroth-order dependence on radical precursor **2b** is not surprising, given that the amount of radicals in solution is dictated by the amount of TBADT photocatalyst, which is present in low concentration (generally 5 mol%). We thus focused on the reaction rate's dependence on TBADT, which could give useful information for extrapolating the reaction mechanism. As mentioned before, experiments were performed under saturation of light, so to maximize the amount of excited photocatalyst in solution. When doubling the amount of photocatalyst (10 mol%), no change was observed in the reaction rate (Figure 9). However, lowering the amount of TBADT to 2.5 or 1.25 mol% decreased the rate of the model reaction, indicating a saturation kinetic profile in [TBADT].

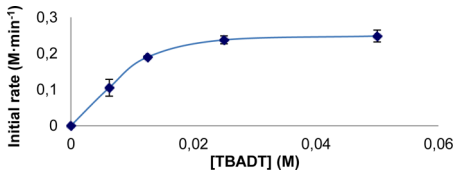

Figure 9. Reaction profile for different initial concentrations of TBADT showing saturation kinetic: [TBADT] = 0.006, 0.0125, 0.025, and 0.05 M. The error bars represent the standard deviation. Model reactions catalyzed by amine **4b** performed under the conditions specified in Figure 7.

Mechanistically, the kinetic order assessment (particularly the TBADT concentration's effect on the reaction rate) can be reconciled with two possible scenarios, characterized by different turnover-limiting steps (see Figure 4 for a full mechanistic picture).

1. On the one hand, lowering the amount of photocatalyst is directly reflected in a lower concentration of reactive open-shell intermediates, since they are generated from substrate **2b** through an HAT mechanism triggered by the photoexcited TBADT. The reduction of the overall reaction rate could be explained in terms of the turnover-limiting step being the radical trapping by the iminium ion **A-1** (the radical conjugate addition step which forms the new carbon−carbon bond while forging the stereogenic center). In this scenario, the strong influence of the catalyst's electronic properties on the reaction rate could be rationalized in terms of the inductive effect of the carbazole moiety influencing the electrophilicity of the iminium ion intermediate **A-1**.[25]
2. On the other hand, less TBADT in solution also means that a lower amount of the reduced photocatalyst (TBADT-H in Figure 4) would be formed upon radical formation (HAT from substrate **2**). TBADT-H is directly involved in the intermolecular SET event that reduces the long-lived carbazoliumyl radical cation in **D-1** to return both the neutral organic catalyst (intermediate **E-1**) and the photoredox catalyst in the original state. This bimolecular SET event, which is essential to close both the iminium ion and the photoredox cycles, could also be the turnover-limiting step of the overall process. This could easily explain the striking correlation (Figures 6c) between the reaction rate and the reduction potential of the carbazole unit tethered to the aminocatalyst **4**.[26] Since the $TBADT^{4-}/TBADT^{5-}$ redox couple is reported at −0.96 V vs Ag/Ag^{+},[27] a larger oxidizing power of the carbazoliumyl radical cation should greatly facilitate the oxidation of TBADT-H by the intermediate **D-1**. This is because the exergonicity of SET from TBADT-H to **D-1** increases when the electron density on the carbazole unit is reduced (**4f** < **4e** < **4g** < **4h**). This was the exact reactivity trend observed in the kinetic studies: for

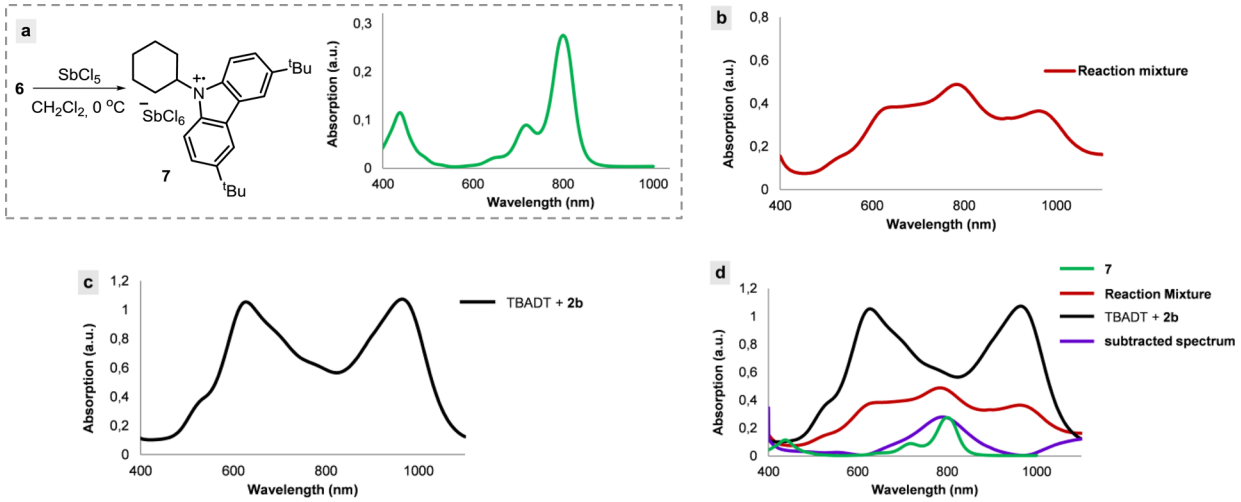

Figure 10. Optical absorption spectra recorded in CH_3CN in 1 mm path quartz cuvettes. (a) Synthesis and spectroscopic characterization of *N*-cyclohexyl carbazoliumyl radical cation **7**. Green spectrum: [**7**] = 0.0004 M in CH_3CN. (b) Red spectrum: mixture containing [**1a**] = 0.03 M, [**4b**] = 0.006 M, [benzoic acid] = 0.006 M, [**2b**] = 0.09 M, $[TBABF_4]$ = 0.03 M and [TBADT] = 0.0015 M dissolved in 1 mL of CH_3CN after 30 min of illumination by a high-power black LED (λ_{max} = 365 nm) with an irradiance of 60 ± 2 mW/cm^2. (c) Black spectrum: mixture containing [**2b**] = 0.09 M, $[TBABF_4]$ = 0.03 M and [TBADT] = 0.0015 M dissolved in 1 mL of CH_3CN after 30 min of illumination by a high-power black LED (λ_{max} = 365 nm) with an irradiance of 60 ± 2 mW/cm^2. (d) Purple spectrum: subtraction of the normalized black spectrum from the red spectrum.

DOI: 10.1021/jacs.7b01446
J. Am. Chem. Soc. XXXX, XXX, XXX−XXX

example, the reaction catalyzed by amine **4h** ($E_{1/2}$ = +1.25 V) is faster than the amine **4f**-mediated process ($E_{1/2}$ = +1.02 V).

Our goal was to unambiguously discriminate between these two possibilities and to eventually ascertain the overall rate-limiting event. The second mechanistic scenario required the bimolecular SET reduction of intermediate **D-1** from the reduced photocatalyst TBADT-H to be turnover-limiting. If this mechanistic hypothesis were to hold true, the intermediate **D-1** would accumulate in solution. In sharp contrast, if the radical trapping from the iminium ion were rate-limiting, it would not be possible to detect any carbazoliumyl radical cation intermediate during the process. We therefore performed further experimental studies to detect the presence of mechanistically relevant transient intermediates in the reaction medium.

Spectroscopic Studies. When treating *N*-cyclohexyl-3,6-di-*tert*-butyl-carbazole **6** with $SbCl_5$, we isolated and characterized the corresponding shelf-stable carbazoliumyl radical cation **7** (Figure 10a). The stability of this intermediate is further evidence of the carbazole radical cation's persistency. **7** shows a characteristic green coloration. Accordingly, its visible absorption spectrum displays a maximum value at 800 nm (green spectrum in Figure 10a). The characteristic absorption of the *N*-cyclohexyl carbazoliumyl radical cation **7** offered an ideal opportunity to check whether a similar intermediate accumulated during the reaction. For this purpose, we recorded the optical absorption spectrum of the reaction mixture. A series of model reactions were performed in CH_3CN under the standard conditions, but in quartz cuvettes. Their absorption spectra were acquired at different irradiation times (a high-power black LED, λ_{max} = 365 nm, with an irradiance of 60 ± 2 mW/cm^2 was used as light source). In all cases, even after an irradiation time as short as 10 min, the absorption spectra of the overall reaction displayed three maxima in the visible region at 630, 800, and 900 nm (red spectrum in Figure 10b). As a control experiment, the absorption spectrum of an identically irradiated solution containing a mixture of the TBADT photoredox catalyst and the radical precursor **2b** was recorded. It is known that the reduced photocatalyst TBADT-H and its disproportionated byproduct[28] are blue in solution.[27] Accordingly, characteristic peaks were clearly observable in the absorption spectrum of the control experiment, with maxima at 630 and 980 nm (black spectrum in Figure 10c).

Figure 10d provides a direct comparison of the absorption spectra of the reaction mixture and the TBADT absorption (red and black lines, respectively), showing an obvious discrepancy in the form of a new band which is only present when all the reaction components are irradiated together. The purple spectrum in Figure 10d is obtained by subtracting the normalized spectrum obtained after irradiation of TBADT and **2b** (black line) from the spectrum recorded for the irradiated reaction mixture (red line). This new spectrum shows an absorption maximum at 800 nm, which is very reminiscent of the characteristic line shape of the *N*-cyclohexyl-3,6-di-*tert*-butyl-carbazoliumyl radical cation **7** (green spectrum).

We then used theoretical studies (TDDFT method, see Supporting Information for details) to compute the absorption spectrum of intermediate **D-1**, which confirms the intense absorption peak in the red portion of the UV−vis spectrum (Figure 11). The modeled band, centered at 758 nm, compares well with the experimentally observed band (purple line),[29]

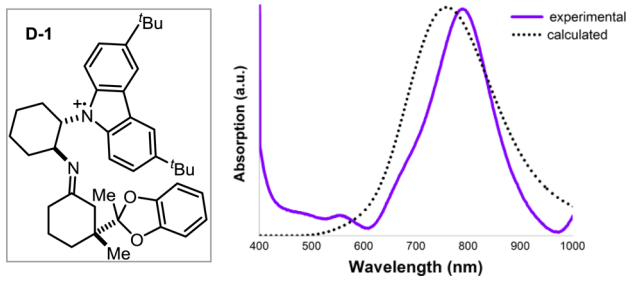

Figure 11. Experimental (purple line) and computed (dotted line) absorption spectra of intermediate **D-1**. The modeled band spectrum in CH_3CN solvent was obtained by a Gaussian convolution (full width at half-maximum of 0.2 eV) of vertical transitions computed at TD-B3LYP/6-31G(d)/PCM level of theory.

providing further support for the carbazoliumyl radical cation intermediate **D-1** being responsible for the peak experimentally observed at ∼800 nm.

Collectively, the spectroscopic studies indicate that the intermediate **D-1** accumulates during the radical conjugate addition process. This behavior is consistent with the overall turnover-limiting step being the reduction of the long-lived carbazoliumyl radical cation in **D-1** to return both the neutral organic catalyst and the TBADT photoredox catalyst in the original state.

CONCLUSIONS

In summary, we have gained a better understanding of the factors governing the iminium ion-mediated radical conjugate addition to *β*,*β*-disubstituted cyclic enones, which set quaternary carbon stereocenters with high fidelity. We have achieved this using a combination of electrochemical, spectroscopic, computational, and kinetic studies. The chemistry exploits the ability of the chiral primary amine catalyst **4**, purposely adorned with a redox-active carbazole moiety, to drive the stereoselective interception of photochemically generated carbon-centered radicals by means of an electron-relay mechanism. An unanticipated turnover-limiting step has been uncovered, for it is the reduction of the carbazole radical cation within intermediate **D-1** and the regeneration of the TBADT photocatalyst that dictate the overall rate of the process. In line with this mechanistic framework, the carbazoliumyl radical cation was detected by visible absorption spectrophotometry in the reaction mixture, thus indicating that this species accumulates before the reaction's slow step.

The insight that the radical trapping and the enantioselective carbon−carbon bond-forming step is not rate-limiting may pave the way for the mechanistically driven design of the next generation of electron-relay catalysts. In this regard, we have found a strong and predictable correlation between the reaction rate and the reduction potential of the carbazole unit tethered to the aminocatalyst **4**. The knowledge that the redox properties can be rationally tuned for improving catalytic activity may enable the development of new iminium ion-mediated asymmetric RCA of highly reactive open-shell intermediates. Our ongoing efforts are directed toward the realization of these aims.

ASSOCIATED CONTENT

Supporting Information

The Supporting Information is available free of charge on the ACS Publications website at DOI: 10.1021/jacs.7b01446.

DOI: 10.1021/jacs.7b01446
J. Am. Chem. Soc. XXXX, XXX, XXX−XXX

Complete experimental procedures, characterization data, and details on kinetic, computational, and spectroscopic studies, including Figures S1−S17 (PDF)

AUTHOR INFORMATION

Corresponding Author

*pmelchiorre@iciq.es

ORCID

Paolo Melchiorre: 0000-0001-8722-4602

Notes

The authors declare no competing financial interest.

ACKNOWLEDGMENTS

Financial support was provided by the Generalitat de Catalunya (CERCA Program), MINECO (CTQ2016-75520-P and Severo Ochoa Excellence Accreditation 2014-2018, SEV-2013-0319), and the European Research Council (ERC 681840 - CATA-LUX). A.B. is grateful to the MECD for a FPU fellowship (ref. FPU13/02402). J.J.M. thanks the Marie Curie COFUND action (291787-ICIQ-IPMP) for a postdoctoral fellowship. The authors thank Dr. David Bastida for useful discussions.

REFERENCES

(1) For pioneering studies on iminium-ion-mediated catalysis, see: (a) Ahrendt, K. A.; Borths, C. J.; MacMillan, D. W. C. *J. Am. Chem. Soc.* **2000**, *122*, 4243−4244. (b) Northrup, A. B.; MacMillan, D. W. C. *J. Am. Chem. Soc.* **2002**, *124*, 2458−2460.

(2) (a) Lelais, G.; MacMillan, D. W. C. *Aldrichimica Acta* **2006**, *39*, 79−87. (b) Erkkilä, A.; Majander, I.; Pihko, P. M. *Chem. Rev.* **2007**, *107*, 5416−5470. For general reviews on organocatalysis, see: (c) MacMillan, D. W. C. *Nature* **2008**, *455*, 304−308. (d) Bernardi, L.; Fochi, M.; Franchini, M. C.; Ricci, A. *Org. Biomol. Chem.* **2012**, *10*, 2911−2922.

(3) Córdova, A., Ed. *Catalytic Asymmetric Conjugate Reactions*; Wiley-VCH: Weinheim, 2010.

(4) (a) Giese, B. *Angew. Chem., Int. Ed. Engl.* **1989**, *28*, 969−980. (b) Srikanth, G. S. C.; Castle, S. L. *Tetrahedron* **2005**, *61*, 10377−10441.

(5) Murphy, J. J.; Bastida, D.; Paria, S.; Fagnoni, M.; Melchiorre, P. *Nature* **2016**, *532*, 218−222.

(6) For reviews discussing catalytic strategies for forging quaternary stereocenters, see: (a) Hawner, C.; Alexakis, A. *Chem. Commun.* **2010**, *46*, 7295−7306. (b) Quasdorf, K. W.; Overman, L. E. *Nature* **2014**, *516*, 181−191. (c) Liu, Y.; Han, S.-J.; Liu, W.-B.; Stoltz, B. M. *Acc. Chem. Res.* **2015**, *48*, 740−751.

(7) Previous examples of metal-catalyzed enantioselective radical conjugate additions to electron-deficient olefins did not provide for the formation of sterically demanding quaternary carbons, see: (a) Sibi, M. P.; Ji, J.; Wu, J. H.; Gürtler, S.; Porter, N. *J. Am. Chem. Soc.* **1996**, *118*, 9200−9201. (b) Sibi, M. P.; Ji, J.; Sausker, J. B.; Jasperse, C. P. *J. Am. Chem. Soc.* **1999**, *121*, 7517−7526. (c) Gansäuer, A.; Lauterbach, T.; Bluhm, H.; Noltemeyer, M. *Angew. Chem., Int. Ed.* **1999**, *38*, 2909−2910. (d) Ruiz Espelt, L.; McPherson, I. S.; Wiensch, E. M.; Yoon, T. P. *J. Am. Chem. Soc.* **2015**, *137*, 2452−2455. (e) Huo, H.; Harms, K.; Meggers, E. *J. Am. Chem. Soc.* **2016**, *138*, 6936−6939.

(8) In general, radical conjugate additions to electron-deficient olefins are rather insensitive to steric hindrance because of the long incipient carbon−carbon forming bond in the early transition state, see: (c) Damm, W.; Giese, B.; Hartung, J.; Hasskerl, T.; Houk, K. N.; Hüter, O.; Zipse, H. *J. Am. Chem. Soc.* **1992**, *114*, 4067−4079. (d) Fischer, H.; Radom, L. *Angew. Chem., Int. Ed.* **2001**, *40*, 1340−1371.

(9) Radical chemistry has found limited application as an enabling strategy for forging quaternary stereogenic centers in a catalytic enantioselective fashion. For selected examples, see: (a) Murakata, M.; Jono, T.; Mizuno, Y.; Hoshino, O. *J. Am. Chem. Soc.* **1997**, *119*, 11713−11714. (b) Zhu, Y.; Zhang, L.; Luo, S. *J. Am. Chem. Soc.* **2014**, *136*, 14642−14645.

(10) Forbes, M. D. *Carbon-Centered Free Radicals and Radical Cations: Structure, Reactivity, and Dynamics*; John Wiley & Sons, Inc.: Hoboken, NJ, 2010.

(11) Jakobsen, H. J.; Lawesson, S. O.; Marshall, J. T. B.; Schroll, G.; Williams, D. H. *J. Chem. Soc. B* **1966**, 940−946.

(12) We chose a chiral primary amine as the iminium ion handle within catalysts **4** because secondary enamines are known to exist mainly as tautomeric electron-poor imines of type **D**. This potentially offered an efficient mechanism to preclude the back-electron transfer between the enamine and the electron hole unit. Rappaport, Z., Ed. *The Chemistry of Enamines*; John Wiley and Sons: Chichester, 1994.

(13) (a) Bollinger, J. M., Jr. *Science* **2008**, *320*, 1730−1731. (b) Okada, Y.; Nishimoto, A.; Akaba, R.; Chiba, K. *J. Org. Chem.* **2011**, *76*, 3470−3476.

(14) The idea of proximity-driven redox processes finds support in the mechanism of electron transfer within biological systems, where even endergonic SET events can be achieved via electron tunneling if the redox centers are in close proximity, see: Page, C. C.; Moser, C. C.; Chen, X.; Dutton, P. L. *Nature* **1999**, *402*, 47−52.

(15) The unique redox properties of carbazoles and the corresponding carbazoliumyl radical cations form the basis of the wide application of carbazole derivatives in hole-transport materials for light-emitting diodes and photovoltaic cells, see: (a) Uoyama, H.; Goushi, K.; Shizu, K.; Nomura, H.; Adachi, C. *Nature* **2012**, *492*, 234−238. (b) Blouin, N.; Leclerc, M. *Acc. Chem. Res.* **2008**, *41*, 1110−1119.

(16) (a) Tzirakis, M. D.; Lykakis, I. N.; Orfanopoulos, M. *Chem. Soc. Rev.* **2009**, *38*, 2609−2621. (b) Ravelli, D.; Protti, S.; Fagnoni, M. *Acc. Chem. Res.* **2016**, *49*, 2232−2242. (c) De Waele, V.; Poizat, O.; Fagnoni, M.; Bagno, A.; Ravelli, D. *ACS Catal.* **2016**, *6*, 7174−7182.

(17) Ravelli, D.; Albini, A.; Fagnoni, M. *Chem. - Eur. J.* **2011**, *17*, 572−579.

(18) In addition to modulating the redox properties of the carbazole scaffold, introducing substituents at the 3- and 6-positions can further stabilize the carbazole radical cation, see: Prudhomme, D. R.; Wang, Z.; Rizzo, C. J. *J. Org. Chem.* **1997**, *62*, 8257−8260 Concurrently, the increased steric hindrance carries the additional benefit of inferring a higher stereocontrol, as evinced when using the highly encumbered primary amine catalyst **4c**.

(19) For an overview of the relevance of apparent outliers in mechanistically interrogating asymmetric catalytic processes, see: Sigman, M. S.; Harper, K. C.; Bess, E. N.; Milo, A. *Acc. Chem. Res.* **2016**, *49*, 1292−1301.

(20) The use of benzodioxole **2a** as the radical precursor (chemistry detailed in Figure 3a) resulted in a slow but detectable background process, with the product **3a** being obtained in ∼10% yield after 15 h in the absence of any catalyst **4**.

(21) In the original study (ref 5), 40 mol% of benzoic acid was used to accelerate the formation of iminium ion (the reaction does not proceed at all without the acid). A careful analysis conducted before the kinetic investigations revealed that the amount of acid could be halved without affecting the reaction rate.

(22) The original study (ref 5) provided a model for rationalizing how the steric hindrance of the carbazole unit affects the stereocontrol. The chiral iminium ion **A** was generated upon condensation of catalyst **4b** and substrate **1a**. The X-ray single-crystal structural analysis of **A** showed a (*Z*)-configuration of the C═N double bond as originating from a stabilizing intramolecular charge transfer π-π interaction between the electron-rich carbazole nucleus and the electron-deficient iminium ion. NMR spectroscopic analyses confirmed that this highly organized topology is also dominant in solution. It likely governs the stereocontrol in the radical conjugate addition. This is because the bulky carbazole unit is positioned in such a way as to effectively shield the *Si* face of the iminium ion, leaving the *Re* face exposed for enantioselective bond formation.

DOI: 10.1021/jacs.7b01446
J. Am. Chem. Soc. XXXX, XXX, XXX−XXX

(23) (a) Schreck, J. O. *J. Chem. Educ.* **1971**, *48*, 103−107. (b) For the seminal report of a linear free energy relationship (LFER) in asymmetric catalysis, see: (b) Jacobsen, E. N.; Zhang, W.; Güler, M. L. *J. Am. Chem. Soc.* **1991**, *113*, 6703−6704.
(24) Hickey, D. P.; Schiedler, D. A.; Matanovic, I.; Doan, P. V.; Atanassov, P.; Minteer, S. D.; Sigman, M. S. *J. Am. Chem. Soc.* **2015**, *137*, 16179−16186.
(25) Since the transmission of polar effects through σ-bonds dies out over short distances (the iminium ion nitrogen in **A-1** is three σ-bonds away from the nitrogen carbazole), a more plausible explanation for why the carbazole electronic properties influence the reaction rate can be as follows: we have already shown that the electron-rich carbazole unit is engaged in a charge-transfer interaction with the LUMO of **A-1** (see refs 5 and 22). The observed reaction behavior may then be explained by a drop in donation of electron density from the carbazole-bearing electron-withdrawing substituents into the LUMO of the iminium ion. This would increase the electrophilicity of **A-1** accelerating the radical trap and the carbon-carbon bond formation.
(26) This scenario could also explain the observed positive linear correlation between the rate constants and the Hammett σ_{para} value of the aryl moiety in catalysts **4e−h** (Figure 6b) due to the loss of positive charge associated with the reduction of the carbazoliumyl radical cation in **D-1** which regenerates the neutral organic catalyst.
(27) Yamase, T.; Takabayashi, N.; Kaji, M. *J. Chem. Soc., Dalton Trans.* **1984**, 793−799.
(28) (a) Renneke, R. F.; Pasquali, M.; Hill, C. L. *J. Am. Chem. Soc.* **1990**, *112*, 6585−6594. The nature of the active species generated after the excitation of TBADT is a matter of current debate, see: (b) Ravelli, D.; Dondi, D.; Fagnoni, M.; Albini, A.; Bagno, A. *Phys. Chem. Chem. Phys.* **2013**, *15*, 2890−2896.
(29) The discrepancy between the computed vertical and the experimental excitations is 0.09 eV. This value fits with the threshold mean absolute error (MAE) associated with the functional adopted herein, which results to be 0.25 eV, see: Jacquemin, D.; Wathelet, V.; Perpète, E. A.; Adamo, C. *J. Chem. Theory Comput.* **2009**, *5*, 2420−2435.

DOI: 10.1021/jacs.7b01446
J. Am. Chem. Soc. XXXX, XXX, XXX−XXX